Accepted Manuscript

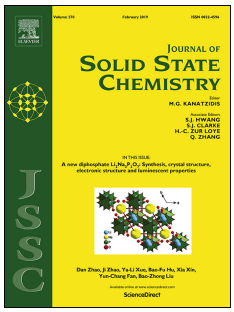

1D lanthanide coordination polymers based on lanthanides and 4'-hydroxi-4-biphenylcarboxylic acid: Synthesis, structures and luminescence properties

Richard F. D'Vries, German E. Gomez, Lina Paola Mondragon, Diego Onna, Beatriz C. Barja, Galo J.A.A. Soler-Illia, Javier Ellena

PII: S0022-4596(19)30104-5

DOI: https://doi.org/10.1016/j.jssc.2019.02.043

Reference: YJSSC 20642

To appear in: *Journal of Solid State Chemistry*

Received Date: 24 January 2019

Revised Date: 26 February 2019

Accepted Date: 27 February 2019

Please cite this article as: R.F. D'Vries, G.E. Gomez, L.P. Mondragon, D. Onna, B.C. Barja, G.J.A.A. Soler-Illia, J. Ellena, 1D lanthanide coordination polymers based on lanthanides and 4'-hydroxi-4-biphenylcarboxylic acid: Synthesis, structures and luminescence properties, *Journal of Solid State Chemistry* (2019), doi: https://doi.org/10.1016/j.jssc.2019.02.043.

TOC

1D lanthanide coordination polymers based on lanthanides and 4'-hydroxi-4-biphenylcarboxylic acid: synthesis, structures and luminescence properties

Richard F. D'Vries[a]*, German E. Gomez[bc]*, Lina Paola Mondragon[a], Diego Onna[cd], Beatriz C. Barja[d], Galo J. A. A. Soler-Illia[c] and Javier Ellena[e]

J. Sol. Stat. Chem., **2019,**

A new family of 1D coordination polymers with formula $[Ln(4\text{-}OHBBA)_3(H_2O)_2]$ and a new 3D supramolecular network topology was obtained. Photoluminescence and sensing tests of doped compounds were performed.

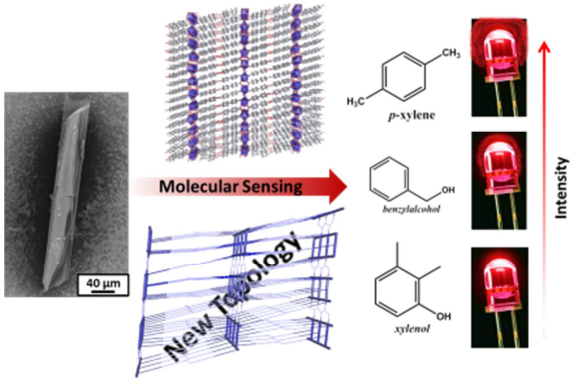

1D lanthanide coordination polymers based on lanthanides and 4'-hydroxi-4-biphenylcarboxylic acid: synthesis, structures and luminescence properties

Richard F. D'Vries[a]*, German E. Gomez[bc]*, Lina Paola Mondragon[a], Diego Onna[cd], Beatriz C. Barja[d], Galo J. A. A. Soler-Illia[c] and Javier Ellena[e]

[a]Facultad de Ciencias Básicas, Universidad Santiago de Cali, Calle 5 # 62-00, Cali, Valle del Cauca, Colombia

[b]Centro Atómico Constituyentes, Comisión Nacional de Energía Atómica (CAC-CNEA), Av. Gral. Paz 1499, 1650 San Martín, Buenos Aires, Argentina

[c]Instituto de Nanosistemas., Universidad Nacional de San Martín (INS-UNSAM), Av. 25 de Mayo 1021, San Martín, Buenos Aires, Argentina

[d] Instituto de Química, Física de los Materiales, Medioambiente y Energía (INQUIMAE-CONICET), DQIAQF, Universidad de Buenos Aires, Ciudad Universitaria, C1428EHA-Buenos Aires, Buenos Aires, Argentina

[e]Instituto de Física de São Carlos, Universidade de São Paulo, A. Trabalhador São-carlense, nº 400 Parque Arnold Schimidt, São Carlos, São Paulo, 13566-590, Brazil

Correspondence email: richard.dvries00@usc.edu.co; gegomez@unsl.edu.ar

Synopsis A family of coordination polymers with formula $[Ln(4\text{-}OHBBA)_3(H_2O)_2]$ with a new 3D supramolecular network topology was obtained. Luminescence properties were studied.

Resume A new family of 1D coordination polymers (CPs) based on 4'-hydroxi-4-biphenylcarboxylic acid (4-OHBBA) linker and lanthanide metals were obtained by hydrothermal synthesis. The compounds were fully characterized and present the general formula $[Ln(4\text{-}OHBBA)_3(H_2O)_2]$ (where Ln= La, Pr), crystallizing in the monoclinic $P2_1/c$ space group. The CPs are formed by "fish bone-like" chains along [010] direction. Also, the topological analysis revels a 3D supramolecular structure with a 7-nodal 3,3,3,4,4,4,4-connected network and the $(6.8^2)^2(6^2.8)^2(6^3.8^2.10)^2(6^3)^4(6^5.8)^2(8^6)$ point symbol. The luminescence and chemical sensing tests of the europium doped compound was performed, finding that the Eu, Tb and Dy -doped samples exhibited dual emissions from the 4-OHBBA ligand and the lanthanide centres.

Keywords: Coordination Polymers; Supramolecular Topology; Lanthanide Metals; Luminescence.

1. Introduction

The study of coordination polymers (CPs) based materials has become a mature field with intense development due to their emerging applications in areas such as catalysis [1, 2], ion exchange [3], gas separation [4], magnetism [5], luminescence [6-8], and antibacterial properties [9]. The possibility of employing a diversity of metals and ligands as building blocks, allows chemists to study specific and unique properties from a rational design [10, 11]. In this sense, lanthanide ions are of special interest in photonics and magnetism because of their unique properties, which include narrow 4f-4f transitions (except La^{3+} and Lu^{3+}) accompanied with a wide lifetime range and high quantum yields [12-15]. These features are important for the design of new phosphors [16], optical amplifiers [17], the generation and amplification of light in lasers [18], solid-state lighting (SSL), full colour displays and backlights [19-21]. Moreover, CPs *hypersensitive transitions* [7, 22, 23] enable Ln-CPs for the construction of sensors for toxic substances [24] or for obtaining radiometric thermosensors [6, 25, 26].

A careful selection of rigid and flexible aromatic linkers has been a key factor to design a diversity of CPs and metal-organic frameworks (MOFs) with original topological architectures [27, 28]. For luminescence properties, the choice of aromatic ligands allows energy transfer processes between the metallic centres and the ligands. In this opportunity, we present the structure elucidation of a new set of 1D Ln-CPs based on 4'-hydroxi-4-biphenylcarboxylic acid (4-OHBBA) with the general formula $[Ln(4\text{-}OHBBA)_3(H_2O)_2]$ (Ln^{3+}=La, Pr), by single X-ray diffraction (SCXRD). The solid samples were also characterized by vibrational and thermal analysis, powder X-ray diffraction (PXRD) and scanning electronic microscopy (SEM). Moreover, an in-depth topological analysis of the Ln-CP compounds was carried out leading to a new description based on predominant H-bonds into the layers, finding a new supramolecular topology. A complementary analysis of the luminescence properties of the Ln-CPs compounds in solid state was explored, presenting the luminescence of the free ligand for the first time. Moreover, sensing assays in presence of "explosive-like" substances were performed in order to study Ln-CPs behaviour as selective chemical sensors.

2. Experimental Section

2.1. General information

All reagents and solvents employed were commercially available and used as supplied without further purification: 4'-hydroxi-4-biphenylcarboxylic acid (4-OHBBA) (99%, Sigma-Aldrich); $Ln(NO_3)_3{\cdot}6H_2O$ where Ln = La and Pr, (99%, Sigma-Aldrich). Thermogravimetric analysis (TGA) was performed using Shimadzu TGA-50 equipment at 25-900˚C temperature range, under nitrogen atmosphere (100 mL/min flow) and $10^{\circ}C{\cdot}min^{-1}$ heating rate. Fourier Transform Infrared spectra were recorded from KBr pellets in the 4000-250 cm^{-1} range on a Bomem Michelson FT MB-102. X-ray powder diffraction (PXRD) patterns were obtained with a Rigaku

Ultima IV diffractometer of 0.02˚ step size and 2 second/step exposure time. The measurements were used to prove the isostructural series, checking the purities of the microcrystalline products obtained by the comparison of experimental and simulated pattern (Supp. Inf. S1). Samples were placed on an adhesive carbon tape coated with gold and micrographs were obtained on FEI Quanta 200 SEM equipment.

2.2. Single-Crystal structure determination

Single-crystal X-ray data for both compounds were collected at room temperature (298 K) on a Bruker APEX-II CCD diffractometer using MoKα radiation (0.71073 Å) and applying a graphite monochromator. The cell determination and the final cell parameters were obtained on all reflections using the software Bruker SAINT included in APEX2 software suite [29]. Data integration and scaled were carried out using also the software Bruker SAINT [30]. The structures were solved by SHELXS-2013 software and then refined by SHELXL-2013 [31], included in WinGX [32] and Olex2 [33]. Non-hydrogen atoms of the molecules were clearly resolved and their full-matrix least-squares refinement with anisotropic thermal parameters were conducted. All hydrogen atoms were stereochemically positioned and refined by the riding model [31]. Hydrogen atoms of the water molecules were localized and fixed (with Uiso(H) = 1.5Ueq) on the density map. Diamond [34], TOPOS [35] andMercury [36] programs were used in the preparation of the artwork of ORTEP diagram, polyhedral and topological representations.

2.3. Luminescence studies

The emission spectra were recorded on a PTI QuantaMaster QM-1 luminescence spectrometer. A 75 W Xenon lamp was used as the excitation source. For the excitation–emission spectra, samples were measured in solid state and methanolic suspensions (0.8 mg of compound in 2 mL of MeOH). Prior to the luminescent studies, the closed glass vials containing the samples were ultrasonicated for 10 minutes to obtain homogeneous suspensions. The slit widths for excitation and emission were 0.5 and 1.5 nm respectively. Luminescence spectra were recorded at room temperature between 380 and 750 nm range, all with identical operating conditions. The data were collected at 0.2 seconds per nm. The sensing activity of $[La_{0.9515}Eu_{0.0485}(4\text{-}OHBBA)_3(H_2O)_2]$ (**1-(5%Eu**)) was investigated monitoring the emission spectra at 611 nm (λ_{exc}= 300 nm). The sensing systems were prepared by introducing 0.8 mg of **1-(5%Eu)** powder into 2 mL of methanol and then adding gradually 250-1000 μL of xylene, xylenol, or benzyl alcohol, for each experiment.

Principal component analysis (PCA) [37] was employed to classify the different analytes using the emission spectra, with MATLAB (for more information see Sup. Inf. S6). The emission spectra were pre-processed, as shown in the Supplementary Information S6. The spectra were

normalized by the maximum emission value of the CPs. Then the spectra were divided in two sections, (i) ligand emission from 390 nm to 560 nm and (ii) europium emission from 560 nm to 710 nm. For the second section, the ligand emission was subtracted, and then multiplied by a factor of 80.

2.4. Synthesis

Several synthetic conditions were explored (See Supp. Inf. Table S1.). The molar composition of the initial reaction mixture in 4-OHBBA$^-$:Ln^{3+}: 108H_2O:86EtOH was fixed. The optimized synthesis procedure is described as follows:

[La(4-OHBBA)$_3$(H_2O)$_2$] (**1**) was obtained by the addition of 4-OHBBA (0.025 g, 0.115 mmol) in 5 mL of ethanol, into a solution of La(NO_3)$_3$·6H_2O (0.05 g, 0.115 mmol) in 5 mL of distilled water. The reaction mixture was adjusted to pH≈6 by the addition of NaOH 1M, under constant stirring at room temperature for 30 minutes. The reaction mixture was then placed in a Parr Teflon-lined stainless-steel autoclave at 160˚C for 17 hours. After slow cooling to room temperature, the crystalline products were filtered and washed with water and ethanol (yield= 47.7%). The same procedure was conducted for the synthesis of [Pr(4-OHBBA)$_3$(H_2O)$_2$] (**2**) where green needle crystals were obtained (yield%=53). The procedure for the synthesis of 5% lanthanide doped samples [from now on referred as **1-(5%Ln)**] was performed as follows: to obtain the doped compound **1-(5%Eu)**, a mixture of 4-OHBBA (0.025 g, 0.115 mmol) in 5 mL of ethanol was added to a dissolution of La(NO_3)$_3$·6H_2O (0.05 g, 0.115 mmol) and Eu(NO_3)$_3$·6H_2O (0.0025 g, 0.0058 mmol) in 5 mL of water. The reaction mixture was adjusted to pH≈6 by the addition of NaOH 1M, under constant stirring for 30 minutes. The reaction mixture was also placed in a Parr Teflon-lined stainless-steel autoclave for reacting under hydrothermal conditions at 160˚C for 20 hours. The crystalline product was obtained as reaction product (yield=43%). Similar procedure was followed in order to obtain the doped phases [$La_{0.9513}Tb_{0.0487}$(4-OHBBA)$_3$(H_2O)$_2$], **1-(5%Tb)**, and [$La_{0.951}Dy_{0.0490}$(4-OHBBA)$_3$(H_2O)$_2$], **1-(5%Dy)**. The metallic content was determined by Inductively Coupled Plasma atomic emission spectroscopy (ICP-AEE), where the final values of Eu, Tb and Dy were around **5**%.

3. RESULTS AND DISCUSSION

3.1. Synthetic analysis and structural description

Different synthesis experiments were carried out to obtain pure phases employing selected lanthanide metals (Supp. Inf. Table S1). Pure phases of the [Ln(4-OHBBA)$_3$(H_2O)$_2$] (namely phase **1**) were only achieved using La and Pr as metallic centres. From the optimized hydrothermal conditions, “needle-shape” crystals (La and Pr phases) were assessed (Figure 1a).

A single crystal and large fractured crystals were obtained from the reaction bulk. Micrographs from the reaction product are depicted in Figure 1.

The use of Nd, Tb and Eu metals resulted in the appearance of an unidentified phase (See Sup. Inf. S1, microcrystalline powder (Figure 1b)). A strategy to cope with this situation and then obtaining luminescencent materials is doping the La-Phase 1 with Eu, Tb and Dy. Doping experiments showed that the addition of 5% of Eu, Tb and Dy metals does not affect the structure. Doping values above 5%, give rise to mixtures of phases.

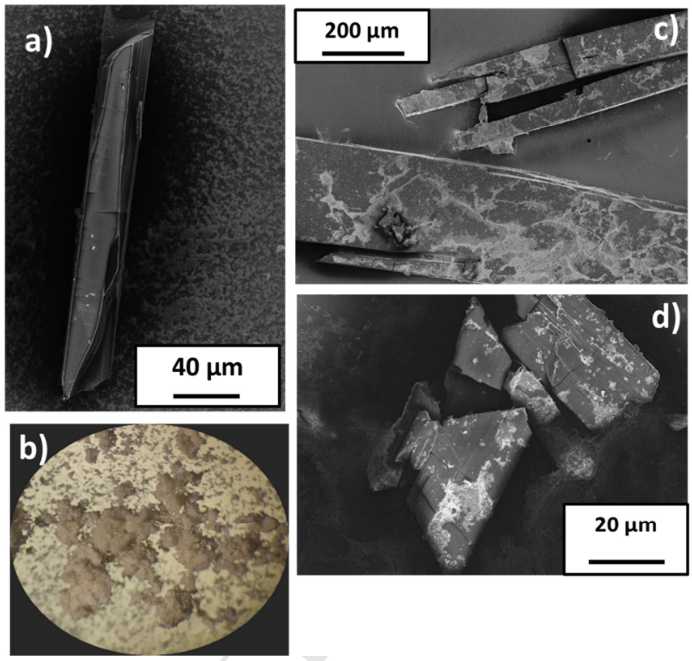

Figure 1 a) Micrographs of bars-like crystals for compound **2** and b) powder product obtained for Tb compound (unknown phase). c) and d) fractured single crystals of the compound 2.

[Ln(4-OHBBA)$_3$(H_2O)$_2$] (Ln = La and Pr) compounds belong to an isostructural family of CPs that crystallized in the monoclinic $P2_1/c$ space group. Details of the data collection and refinement for both compounds are summarized in Table 1. The ORTEP diagram for compound **1** is shown in Figure 2.

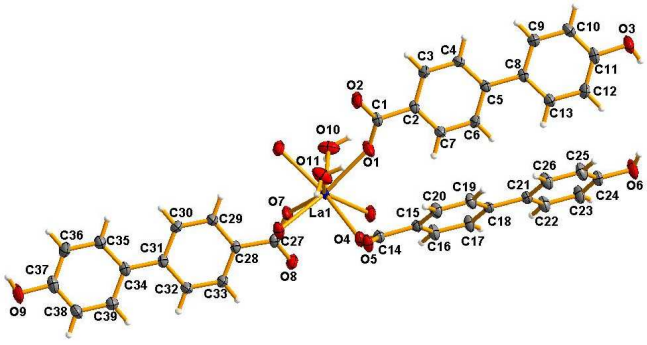

Figure 2 ORTEP diagram of compound **1** showing 50% of probability ellipsoids.

Table 1 Crystallographic data and refinement parameters for **1** and **2** compounds.

Compound	**1**	**2**
Emp. Formula	$C_{39}H_{31}O_{11}La$	$C_{39}H_{31}O_{11}Pr$
FW ($g \cdot mol^{-1}$)	814.55	816.55
Temp. (K)	298	298
λ (Å)	0.71073	0.71073
Crystal system	Monoclinic	
Space Group	$P2_1/c$	
Unit cell		
a (Å)	24.6468(9)	24.6066(1)
b (Å)	5.4670(2)	5.4449(2)
c (Å)	23.4077(8)	23.2997(1)
β (˚)	94.252(1)	94.007(1)
Volume ($Å^3$)	3145.4(2)	3114.1(3)
Z	4	4
ρ_{calc} ($mg \cdot m^3$)	1.720	1.742
Abs.Coeff. (mm^{-1})	1.428	1.635
F(000)	1864	1648
θ range (˚)	1.7 - 26.5	1.7 - 27.6
Reflections collected / Unique [R(int)]	60811/6510 [0.041]	13511/6794 [0.032]
Completeness (%)	99.6	94.2
Data / restraints / parameters	6510/0/465	6794/0/465
Gof on F^2	1.06	1.03

R1 [I>2σ(I)]	0.0229	0.0326
wR2[I>2σ(I)]	0.0575	0.0833

The asymmetric unit consists in a unique metallic centre, three 4-OHBBA ligands and two coordinated water molecules. The primary building unit (PBU) consists of an 8-coordinated polyhedral (LnO_8) with six oxygen atoms belonging to the carboxylate groups and two oxygen from coordinated water molecules adopting a distorted trigonal prism square-face bicapped geometry (TPRS-8) [38] (Figure 3). The carboxylate group in the three crystallographically independent 4-OHBBA ligand exhibits a bidentate-bridge $\mu\eta^2$ coordination mode. One of them joins two metallic centres along [001] direction, with an intermetallic distance of 5.467(3) Å. The other two carboxylates link the dimeric SBUs along [010] direction (intermetallic distance 5.767(7) Å) to form a "fish bone-like" 1D coordination polymer (Figure 3). According to the connectivities displayed by the organic and inorganic sub-units in the structure, these CPs could be classified as I^1O^0 "inorganic chains," where I^1 means that the inorganic connectivity is 1D, and O^0 implies that the organic one is 0D since organic linkers just coordinate to lanthanide ions without connecting chains. The overall dimensionality of the structure is 1D as the sum of the exponents [39].

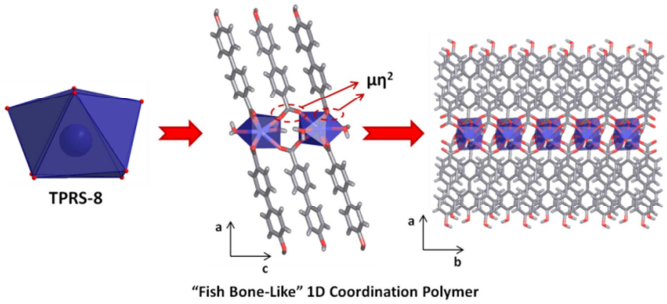

Figure 3 PBU, coordination modes and view along [010] and [001] directions of the [Ln(4-OHBBA)$_3$(H_2O)$_2$] compounds.

Each 1D chain is connected through strong hydrogen bonds [40] between the coordinated water molecules along [001] direction with a distance O-H···O = 2.848 (2) Å (Figure 5). This interaction is repeated along all the structure, forming a C(2) O-H···O-H···O-H chain (Figure 5) and giving rise to the 2D supramolecular structure arranged in the (110) plane. The same connectivity is observed along the [100] where the hydroxyl groups interact between them with a distance O-H···O = 2.944(3) Å, joining the layers along [100] to obtain a 3D supramolecular structure. This supramolecular behaviour should be related to the cleavage properties of the crystal observed in the Figure 1. The strongest direction of the crystal is associated with the growing chains direction along [010] direction, plane (101). The weakest area in the crystal is associated with the planes of the supramolecular layers (100) and (001) (Figure 4).

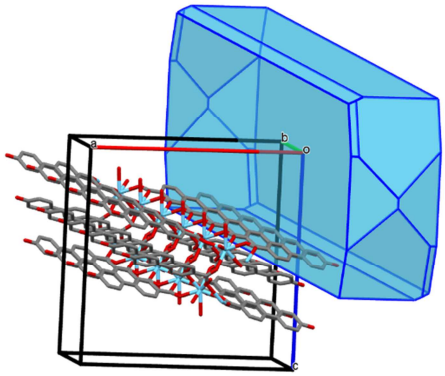

Figure 4. BFDH morphology and unit cell for the compound the [Ln(4-OHBBA)$_3$(H_2O)$_2$].

Deprotonation of the carboxylic acid group and its further coordination to d-transition metals is the only trend observed in all the reported coordination compounds based on 4-OHBBA linker according to the CCDC database [41]. In all the cases, the use of strong bases such as amines or NaOH, is not enough to deprotonate the phenol group and enable the coordination to a metallic centre.

3.2. Topological description

The *underlying topology* was completed by getting a net associated with the structural crystal packing [42]. In this sense, the connectivities of the building blocks were considered to find resemblances or differences among previously reported frameworks. For this purpose, TOPOS program was employed [35]. From the topological point of view, the 2D network was built from the interaction of coordinated water molecules in the “fish bone-like” chains giving rise to layers in the (011) plane. These layers could be simplified considering each metallic centre as a 4-connected nodal point, each water molecule and the ligand as 3-connected and 2-connected linkers respectively. The resulting layers present a binodal network with point symbol ($4^2.5^2.6.7$)(5^3) and **3,4L29** topology (Figure 5) [35]. The supramolecular representation was formed by the interaction between the hydroxyl groups of the 4-OHBBA ligand. These interactions link the layers along [100] direction acting as a 3-connected node giving rise to a 7-nodal 3,3,3,4,4,4,4-connected network with $(6.8^2)^2(6^2.8)^2(6^3.8^2.10)^2(6^3)^4(6^5.8)^2(8^6)$ point symbol. It is worth to underline that the 3D network exhibits a new topology reported here.

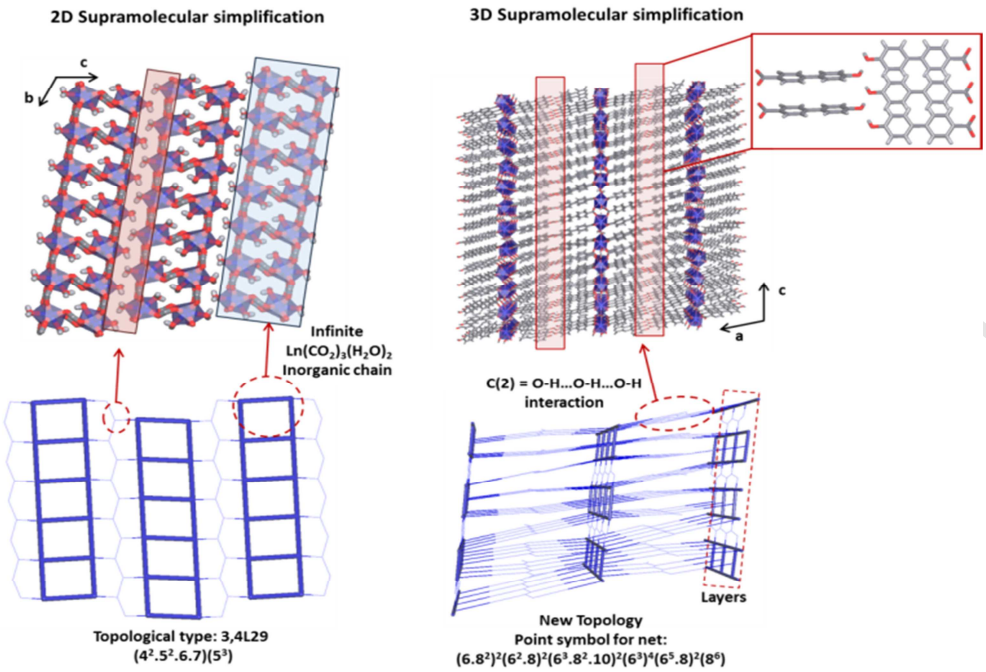

Figure 5 Representation of the ladder form chains and the simplification of the 2D and 3D supramolecular network for the [Ln(4-OHBBA)$_3$(H$_2$O)$_2$] compounds.

3.3. Vibrational behaviour and thermal properties.

Given the isostructural nature of compounds 1 and 2, compound **1** was selected as model to describe their vibrational and thermal properties (Supp. Inf. S2). The interpretation of the FTIR spectra was performed by considering the most important internal vibrations of water molecules, carboxylate and aromatic ring modes and their comparison with those observed in lanthanide-carboxylates networks [43]. νC-H vibrations belonging to aromatic rings of 4-OHBBA ligands were found at around ~ 3030 cm^{-1}. Broad band at approximately ~ 3390 cm^{-1} and small peak at 3590 cm^{-1} were assigned to the νO-H vibration of the coordinated water molecules and from the terminal OH group from 4-OHBBA linker, respectively. Two peaks at 1520 and 1400 cm^{-1} were related to asymmetrical and symmetrical νCOO vibration in a bridging complex [44]. The band in 1255 cm^{-1} was assigned to C-O vibration of the phenyl group.

Thermogravimetric profile for both compounds revealed similar features with a mass loss of 5% (calculated = 4.7 %) (T_{onset} 175 ºC), belonging to coordinated water molecules followed by the total decomposition (T_{onset} 330 ºC) (Supp. Inf. S3). This thermal behaviour showed the important role of the water-water hydrogen bonds in the structural packing and its thermal stability, increasing the water dehydration temperature. Thermal evolution proceeds with the decomposition of the organic portions through two steps leading to the formation of the respective Ln_2O_3.

3.4. Luminescence Properties.

According to current studies, there is an increasing interest regarding to the synthesis and study of luminescent CPs [45], not only from the academic point of view, but also for the potential applications in optical devices for chemical and physical sensors [46]. In this context, luminescent properties of **1**, **2**, **1-(5%Eu)** and **1-(5%Tb)** compounds were explored. As shown in Figure 6a, the linker exhibits a wide blue emission band located at 384 nm (λ_{exc}=300 nm) attributed to the typical $\pi^*\rightarrow\pi/\pi^*\rightarrow$n transitions of aromatic ligands [47]. For this reason, the λ_{exc}=300 nm was selected as excitation wavelength for the rest of the series. The ligand excitation spectrum shows two bands located at 300 and 340 nm (or one band in ethanol solution, Supp. Inf. S4).

The emission spectra of compounds **1** and **2** are mostly dominated by a broad band attributable to $\pi^*\rightarrow\pi$ (or $\pi^*\rightarrow$n) relaxation transitions (see Figure 6b). These bands are blue-shifted from the free-ligand, suggesting *metal-disturbed ligand* transitions [47]. The direct excitation of **1-(5%Eu)** into the Eu^{3+} levels serves as the sensitization pathway to produce 4f emission, where a weak intense signal ascribed to $^5D_0\rightarrow{}^7F_2$ transition was identified (Figure 6c). The doped lanthanide compounds exhibited weak 4f transitions upon excitation at 300 nm where $^5D_4\rightarrow{}^7F_J$ and $^3P_0\rightarrow{}^3H_6$ transitions were located for **1-(5%Tb)** and **2** respectively, as show in Figure 6d and 5e. The quenching effect on the lanthanide emission of doped samples can be explained in terms of the influence of OH from coordinated water molecules and the OH terminal groups of 4-OHBBA (see Supp. Inf. S5), as it was possible to see in lanthanide frameworks [48] [49].

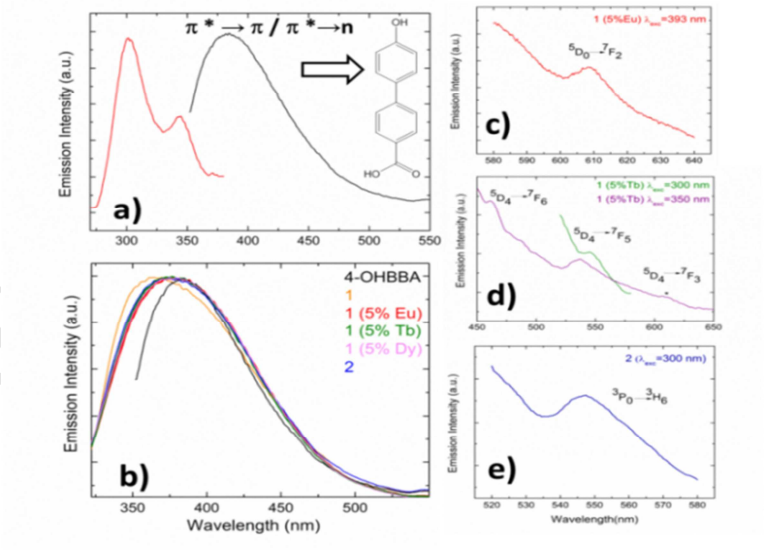

Figure 6 a) Excitation (λ_{em} = 384 nm) and emission spectra (λ_{exc}=300 nm) of 4-OHBBA ligand, b) SSPL of 1 and 2 and the doped 1 (5%Ln, where Ln = Eu, Tb or Dy) compounds in

comparison with the free ligand. Intra-configurational 4f transitions of the respective doped systems (c, d and e).

The $^5D_0 \rightarrow ^7F_2$ *hypersensitive transition* of some Eu-CPs has been useful to sense a variety of chemical entities [50-52]. For this reason, **1-(5%Eu)** was chosen to test the molecule sensing towards aromatic molecules in solutions. Figure 7a shows a set of sensing experiments related along with the concentration of aromatic substances as xylene, xylenol and benzyl alcohol. In Figure 7b, it is clear how the progressive amount of xylene (from 0-1000 μL) increases the ligand emission up to ~35%, while the increase in intensity is less marked in presence of benzylalcohol and xylenol (Figure 7c and d). This phenomenon might be explained in terms of proximities of the electronic levels from the aromatic compounds to the excited states from the linker [8][53]; moreover, the $^5D_0 \rightarrow ^7F_2$ emission located at 610 nm is quenched by the addition of the analytes. This behaviour could be ascribed to the presence of the –OH groups of the analytes under study.

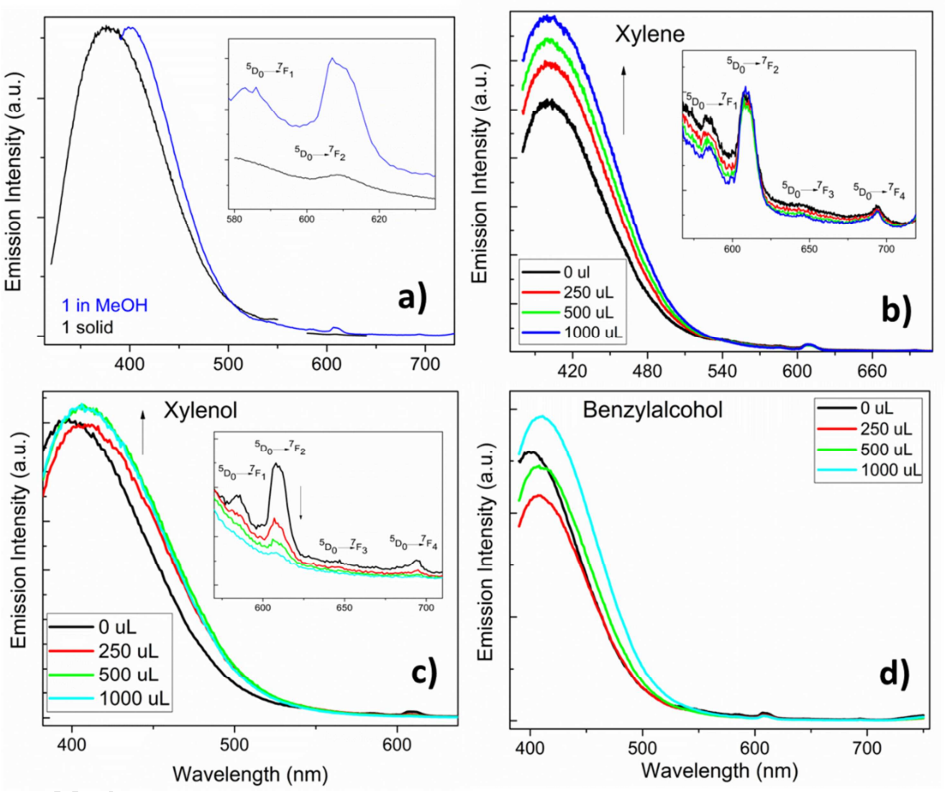

Figure 7 a) PL performance of compound 1 in MeOH and the optical responses of 1-(5%Eu) in presence of 0-1000 μL of b) xylene, c) xylenol and d) benzylalcohol.

PCA was employed taking into account both signal contributions from the sensor (ligand emission at 384 nm and the europium emission at 610 nm) and for classifying the type of analytes) [54]. PCA is a commonly used tool in unsupervised classification, which can extract the dominant patterns in the data based on their similarity without any prior knowledge of their

classification (see details in Supp. Inf. S6). The emission spectra were pre-processed, as detailed in the Supp. Inf. S7, before applying the PCA routine. The two most relevant components that PCA provided explain 86.8% of the variation. The scores plot for these two components, PC1 versus PC2, is shown in Supp. Inf. S8. PCA analysis revealed a clear discrimination of the analytes between the three groups, which is a function of the principal component variation in the samples, based on their chemical structure. The three groups are: (i) the xylene with only methyl group, (ii) the xylenol with methyl and hydroxyl groups and, (iii) the benzyl alcohol with hydroxymethyl group. These results give promising findings for the use of CPs as sensors for explosives precursors.

4. Conclusions

A new set of new CPs based on 4'-hydroxi-4-biphenylcarboxylic acid (4-OHBBA) with lanthanides (La and Pr) was obtained by hydrothermal conditions and fully characterized by powder and single crystal X-ray diffractions, vibrational and thermal analysis. The compounds, with general formula $[Ln(4\text{-}OHBBA)_3(H_2O)_2]$, were characterized as one-dimensional inorganic chains structure along [010] direction. Their metallic coordination spheres were octa-coordinated and incorporate two water molecules in the asymmetric units. The supramolecular topology of a coordination polymer as a 7-nodal 3,3,3,4,4,4,4-connected network with point symbol $\mathbf{(6.8^2)^2(6^2.8)^2(6^3.8^2.10)^2(6^3)^4(6^5.8)^2(8^6)}$ was described for the first time in this study. Besides, the solid-state photoluminescence (SSPL) analysis of the sample set was carried out in terms of absorption, excitation and emission studies. The Eu, Tb and Dy -doped samples exhibited dual emissions from the 4-OHBBA ligand and the lanthanide ones, whose 4f quenching is explained in terms of OH relaxation pathways. Finally, sensing experiments employing the Eu-doped sample showed promising perspectives for the differential response under the presence of "explosive-like" molecules such as xylene, xylenol and benzyl alcohol.

Acknowledgements R. D. acknowledges Coordenação de Aperfeiçoamento de Pessoal de Nivel Superior for the CAPES/PNPD scholarship from the Brazilian Ministry of Education. R. D. and L. P. M. acknowledges to the Dirección General de Investigaciones from Universidad Santiago de Cali for the financial support (project No 939-621118-37). J. E. is grateful to CNPq for the research fellowships. D. O. and G. E. G. acknowledge CONICET for postdoctoral fellowships. G. E. G., G. J. A. A. S. I. and B. C. B. are members of CIC-CONICET.

References

[1] J.-L. Wang, C. Wang, W. Lin, ACS Catal., 2 (2012) 2630-2640.
[2] A. Corma, H. García, F.X. Llabrés i Xamena, Chem. Rev., 110 (2010) 4606-4655.

[3] S.-S. Chen, P. Wang, S. Takamizawa, T.-a. Okamura, M. Chen, W.-Y. Sun, Dalton Trans., (2014).
[4] J.-R. Li, J. Sculley, H.-C. Zhou, Chem. Rev., 112 (2011) 869-932.
[5] G. Minguez Espallargas, E. Coronado, Chem. Soc. Rev., 47 (2018) 533-557.
[6] R.F. D'Vries, S. Alvarez-Garcia, N. Snejko, L.E. Bausa, E. Gutierrez-Puebla, A. de Andres, M.A. Monge, J. Mater. Chem. C, 1 (2013) 6316-6324.
[7] (a) R.F. D'Vries, G.E. Gomez, J.H. Hodak, G.J.A.A. Soler-Illia, J. Ellena, Dalton Trans., 45 (2016) 646-656. (b) M. C. Bernini, G. E. Gomez, E. V. Brusau, G. E. Narda, Isr. J. Inorg. Chem., (2018), https://doi.org/10.1002/ijch.201800095.
[8] R.F. D'Vries, G.E. Gomez, D.F. Lionello, M.C. Fuertes, G.J.A.A. Soler-Illia, J. Ellena, RSC Adv., 6 (2016) 110171-110181.
[9] G.E. Gomez, R.F. D'Vries, D.F. Lionello, L.M. Aguirre-Diaz, M. Spinosa, C.S. Costa, M.C. Fuertes, R.A. Pizarro, A.M. Kaczmarek, J. Ellena, L. Rozes, M. Iglesias, R. Van Deun, C. Sanchez, M.A. Monge, G.J.A.A. Soler-Illia, Dalton Trans., 47 (2018) 1808-1818.
[10] N. Snejko, C. Cascales, B. Gomez-Lor, E. Gutierrez-Puebla, M. Iglesias, C. Ruiz-Valero, M.A. Monge, Chem. Commun., (2002) 1366-1367.
[11] C. Wang, T. Zhang, W. Lin, Chem. Rev., 112 (2011) 1084-1104.
[12] J.-C.G. Bünzli, S. Comby, A.-S. Chauvin, C.D.B. Vandevyver, J. Rare Earths, 25 (2007) 257-274.
[13] F. Le Natur, G. Calvez, C. Daiguebonne, O. Guillou, K. Bernot, J. Ledoux, L. Le Pollès, C. Roiland, Inorg. Chem., 52 (2013) 6720-6730.
[14] X. Fan, S. Freslon, C. Daiguebonne, G. Calvez, L. Le Polles, K. Bernot, O. Guillou, J. Mater. Chem. C, 2 (2014) 5510-5525.
[15] P.G. Derakhshandeh, J. Soleimannejad, J. Janczak, A.M. Kaczmarek, K. Van Hecke, R. Van Deun, CrystEngComm, 18 (2016) 6738-6747.
[16] M.H.V. Werts, Sci. Prog. (1933-), 88 (2005) 101-131.
[17] A. Polman, F.C.J.M. van Veggel, J. Opt. Soc. Am. B, 21 (2004) 871-892.
[18] J. Marling, IEEE Journal of Quantum Electronics, 14 (1978) 56-62.
[19] B.W. D'Andrade, S.R. Forrest, Adv. Mater., 16 (2004) 1585-1595.
[20] H.-C. Su, H.-F. Chen, F.-C. Fang, C.-C. Liu, C.-C. Wu, K.-T. Wong, Y.-H. Liu, S.-M. Peng, J. Am. Chem. Soc., 130 (2008) 3413-3419.
[21] Y.H. Niu, M.S. Liu, J.W. Ka, J. Bardeker, M.T. Zin, R. Schofield, Y. Chi, A.K.Y. Jen, Adv. Mater., 19 (2007) 300-304.
[22] J.C.G. Bünzli, C. Piguet, Chem. Soc. Rev., 34 (2005) 1048-1077.
[23] C.D.S. Brites, P.P. Lima, N.J.O. Silva, A. Millan, V.S. Amaral, F. Palacio, L.D. Carlos, New J. Chem., 35 (2011) 1177-1183.
[24] Z. Hu, B.J. Deibert, J. Li, Chem. Soc. Rev., 43 (2014) 5815-5840.
[25] D. Ananias, C.D.S. Brites, L.D. Carlos, J. Rocha, Eur. J. Inorg. Chem., 2016 (2016) 1967-1971.
[26] G. E. Gomez, A. M. Kaczmarek, R. Van Deun, E.V. Brusau, G. E. Narda, D. Vega, M. Iglesias, E. Gutierrez-Puebla, M.Á. Monge, Eur. J. Inorg. Chem., 2016 (2016) 1577-1588.
[27] W. Lu, Z. Wei, Z.-Y. Gu, T.-F. Liu, J. Park, J. Park, J. Tian, M. Zhang, Q. Zhang, T. Gentle Iii, M. Bosch, H.-C. Zhou, Chem. Soc. Rev., 43 (2014) 5561-5593.
[28] A.K. Inge, M. Köppen, J. Su, M. Feyand, H. Xu, X. Zou, M. O'Keeffe, N. Stock, J. Am. Chem. Soc., 138 (2016) 1970-1976.
[29] Bruker-AXS, I. *APEX2 Software Suite*, 2; Madison, WI, 2006.
[30] Bruker-Siemens, I. *SAINT*, V 6.28A; Madison, WI., 1997.
[31] G. Sheldrick, Acta Crystallogr. A, 64 (2008) 112-122.
[32] L. Farrugia, J. Appl. Crystallogr., 45 (2012) 849-854.
[33] O.V. Dolomanov, L.J. Bourhis, R.J. Gildea, J.A.K. Howard, H. Puschmann, J. Appl. Crystallogr., 42 (2009) 339-341.
[34] K. Brandenburg, H. Putz, *DIAMOND- Crystal and Molecular Structure Visualization*, Crystal Impact: Kreuzherrenstr. 102, 53227 Bonn, Germany, 2006.
[35] V.A. Blatov, A.P. Shevchenko, D.M. Proserpio, Cryst. Growth Des., 14 (2014) 3576-3586.

[36] C.F. Macrae, I.J. Bruno, J.A. Chisholm, P.R. Edgington, P. McCabe, E. Pidcock, L. Rodriguez-Monge, R. Taylor, J. Van De Streek, P.A. Wood, J. Appl. Crystallogr., 41 (2008) 466-470.
[37] H. Abdi, L.J. Williams, Wiley Interdisciplinary Reviews: Computational Statistics, 2 (2010) 433-459.
[38] N.G. Connelly, ; Damhus, T.;Hartshorn, R.M.; Hutton, A.T., Nomenclature of Inorganic Chemistry - IUPAC Recommendations 2005, RSC Publishing, Cambridge, UK., 2005.
[39] A.K. Cheetham, C.N.R. Rao, R.K. Feller, Chem. Commun., (2006) 4780-4795.
[40] G.R. Desiraju, T. Steiner, The Weak Hydrogen Bond: In Structural Chemistry and Biology Oxford University Press, USA, 2001.
[41] F. Allen, Acta Crystallogr. B, 58 (2002) 380-388.
[42] E.V. Alexandrov, V.A. Blatov, A.V. Kochetkov, D.M. Proserpio, CrystEngComm, 13 (2011) 3947-3958.
[43] R.F. D'Vries, V.A. de la Peña-O'Shea, N. Snejko, M. Iglesias, E. Gutiérrez-Puebla, M.A. Monge, J. Am. Chem. Soc., 135 (2013) 5782-5792.
[44] K. Nakamoto, in, JOHN WILEY & SONS, INC., Hoboken, New Jersey, 2009.
[45] Y. Cui, Y. Yue, G. Qian, B. Chen, Chem. Rev., 112 (2011) 1126-1162.
[46] Y. Cui, H. Xu, Y. Yue, Z. Guo, J. Yu, Z. Chen, J. Gao, Y. Yang, G. Qian, B. Chen, J. Am. Chem. Soc., 134 (2012) 3979-3982.
[47] W. Chen, J.-Y. Wang, C. Chen, Q. Yue, H.-M. Yuan, J.-S. Chen, S.-N. Wang, Inorg. Chem., 42 (2003) 944-946.
[48] G.E. Gomez, E.V. Brusau, A.M. Kaczmarek, C. Mellot-Draznieks, J. Sacanell, G. Rousse, R. Van Deun, C. Sanchez, G.E. Narda, G.J.A.A. Soler Illia, Eur. J. Inorg. Chem., 2017 (2017) 2321-2331.
[49] X. Guo, G. Zhu, Q. Fang, M. Xue, G. Tian, J. Sun, X. Li, S. Qiu, Inorg. Chem., 44 (2005) 3850-3855.
[50] H. Xu, F. Liu, Y. Cui, B. Chen, G. Qian, Chem. Commun., 47 (2011) 3153-3155.
[51] X. Zhou, H. Li, H. Xiao, L. Li, Q. Zhao, T. Yang, J. Zuo, W. Huang, Dalton Trans., 42 (2013) 5718-5723.
[52] D. Banerjee, Z. Hu, J. Li, Dalton Trans., 43 (2014) 10668-10685.
[53] L.-Y. Pang, G.-P. Yang, J.-C. Jin, M. Kang, A.-Y. Fu, Y.-Y. Wang, Q.-Z. Shi, Cryst. Growth Des., 14 (2014) 2954-2961.
[54] R. Bro, A.K. Smilde, Analytical Methods, 6 (2014) 2812-2831.